Direct Active Stabilization of the DC-Link in Voltage-Source Converters

Matthieu Bertin*, Mohamad Koteich**
*Elsys Design, consultant for Schneider-Toshiba Inverter Europe
**Schneider-Toshiba Inverter Europe
Schneider Electric
27120 Pacy-sur-Eure, France
URL: https://www.se.com/drives

Keywords

≪Voltage-Source Converters≫, ≪DC-Bus≫, ≪Stability Analysis≫, ≪Motor Drives≫

Abstract

This paper presents an active stabilization method of the dc-link voltage in voltage-source converters. It is a direct compensation method, acting on the converter command voltages instead of the current loop reference, which allows for a wider bandwidth. The proposed method is compared to the state-of-the-art direct compensation method, i.e. filtering the dc-voltage used in the pulse-width-modulation process. The effectiveness of the proposed method over the complete operating range is demonstrated with theoretical analysis and simulation results.

Introduction

In voltage-source power converters, such as the Variable Speed Drive (VSD), undamped oscillations of the dc-link deteriorate the performances of the system and may damage the converter [1]. It has been shown that these oscillations can be caused by the control algorithm's design and tuning, which reduces the damping of the dc-link's LC circuit [2].

Most of the active stabilization methods proposed in the literature are based on the Constant-Power Load (CPL) assumption [1, 3, 4, 5]. Although this simplified model is well-suited for control design, more advanced design and tuning require a higher-order model to account for the load dynamics [2, 6, 7, 8]. For both the CPL model and the higher-order model, the stabilization mechanism consists of adding to the load power a component that is proportional to the oscillating dc-voltage signal δv_{dc}. This compensation can be applied indirectly at the input of the (current or power) controller [1, 8], in which case the stabilization controller's bandwidth is limited to the feedback system's bandwidth. Otherwise, it can be applied directly at the output of the controller (voltage command) [4, 9, 10], which allows for wider bandwidth.

In this paper, we only focus on the direct compensation method as it covers a wider range of applications, especially the slim-capacitor VSD [11], where the resonance frequency is in the range of several hundreds, up to several thousands, of hertz. One commonly used direct compensation method is to low-pass filter the dc-voltage used when normalizing the command voltages before the pulse-width-modulation (PWM) process [2, 10]. This method is simple and effective, yet it has not been thoroughly studied in the literature. In this paper, we present a detailed analysis of this method using the small-signal model. It is shown that it acts only on the amplitude of the output voltage, and that the compensation gain is proportional to both the modulation index and the oscillation δv_{dc}. When the output voltage is saturated, the performance deteriorates.

The main contribution of this paper is a new direct compensation method that exploits both the amplitude and the phase of the output voltage. It has two main advantages compared to the state-of-the-art methods:

1) it covers the whole operating range, including voltage saturation (and field-weakening), and 2) it is easier to tune using the virtual capacitance concept (one intuitive tuning parameter), independently of the modulation index.

After this introduction, the dc-link model and stabilization principle are presented in Section 1. The state-of-the-art dc-link voltage filtering method is presented and analyzed in Section 2. In Section 3, the proposed direct method is presented, analyzed, and compared with the state-of-the-art. The results of the theoretical analysis are confirmed by the simulation results.

1 DC-link model and stabilization principle

The equivalent model of the dc-link is nonlinear. It is described as:

$$L_{dc}\frac{di_{src}}{dt} = v_{src} - v_{dc} - R_{dc}i_{src} \tag{1}$$

$$C_{dc}\frac{dv_{dc}}{dt} = i_{src} - \frac{P}{v_{dc}} \tag{2}$$

In this paper, we take the slim-capacitance VSD as an application example. C_{dc} is the (slim) film capacitance, L_{dc} is the grid inductance referred to the dc-link, as there is no dc-choke in the VSD. R_{dc} is the sum of the grid resistance referred to the dc-link and the parasitic resistance due to unmodeled phenomena, such as commutation overlap in the input rectifier. P is the load power (motor and inverter). When the motor is controlled with tight bandwidth control loops, the inverter/motor system is often modeled as a CPL ($P = P_0$, and $\delta P = 0$). In small-signal, around the equilibrium, the model becomes:

$$L_{dc}\frac{d\delta i_{src}}{dt} = \delta v_{src} - R_{dc}\delta i_{src} - \delta v_{dc} \tag{3}$$

$$C_{dc}\frac{d\delta v_{dc}}{dt} = \delta i_{src} - \frac{\delta P}{v_{dc0}} + \frac{P_0}{v_{dc0}^2}\delta v_{dc} \tag{4}$$

Subscript 0 denotes the equilibrium point. The small-signal symbol δ can be omitted in the sequel for simplicity. The model described in equations (3), (4) is prone to instability. The stabilization principle relies on shaping the small-signal behavior of δP so it becomes proportional to the small-signal dc-link voltage $\delta P = K_a \delta v_{dc}$, to compensate for the negative incremental resistance $(-v_{dc0}^2/P_0)$ [2]. K_a is the active damping gain. In practice δv_{dc} is estimated by the high-pass filtered v_{dc}. As the high-pass filter (HPF) approximates the time-derivative in the large-signal domain, this strategy can be interpreted as adding a virtual capacitor C_v in parallel with C_{dc} [3].

Active Stabilization and the Concept of Virtual Capacitance

In a VSD, the power P is not controlled directly. Hence, to shape $P = P_0 + K_a \delta v_{dc}$, the compensation can be performed by acting on:

- the motor current i_s or torque T_e through the control loop (indirect compensation); or
- the output voltage's amplitude, frequency, or phase (direct compensation).

The performance of the active damping can be tuned using the gain K_a. To make this tuning intuitive, we can use the virtual capacitance (C_v) concept presented in [3]; the load power in small-signal is $\delta P = K_a \delta v_{dc}$, where δv_{dc} is equivalent to dv_{dc}/dt in large signal. Let $K_a = C_v v_{dc0}$, the power δP can be interpreted as the power of a virtual capacitance C_v mounted in parallel to C_{dc}. Therefore, the gain K_a can be interpreted as the amount of capacitance to be added to the dc-link.

General Form of Direct Compensation

Direct compensation does not rely on the controller structure or bandwidth. It covers a wider range of resonance frequency as it is limited by the bandwidth of the PWM process instead of the controller. Using complex-vector notation of the output voltage, we propose the following general direct compensation expression (δV_s, $\delta\omega_s$ and $\delta\phi_v$ are proportional to δv_{dc}):

$$\underline{v}_s = (V_s + \delta V_s)e^{j[(\omega_s+\delta\omega_s)t+(\phi_v+\delta\phi_v)]} \tag{5}$$

Where V_s, ω_s, and ϕ_v, are respectively the amplitude, angular frequency, and phase, of the command voltage. This general expression is thoroughly studied in section 3.

2 DC-link Voltage Filtering-based Stabilization

The voltage command at the output of the controller, $\underline{v}_s^* = V_s e^{j(\omega_s t+\phi)}$, is divided by v_{dc} to calculate the duty-cycles of the inverter switches. One common active stabilization method consists of low-pass filtering v_{dc} used in normalization. Taking $v_{dc}^* = LPF\{v_{dc}\} \approx v_{dc} - \delta v_{dc}$, the normalized voltage becomes:

$$\underline{m}_s = \frac{\underline{v}_s^*}{v_{dc}^*} = \frac{V_s}{v_{dc}-\delta v_{dc}} e^{j(\omega_s t+\phi)} = \frac{V_s/v_{dc}}{1-\delta v_{dc}/v_{dc}} e^{j(\omega_s t+\phi)} \tag{6}$$

In Eq. (6), $\delta v_{dc} << v_{dc}$. Using the first-order approximation $1/(1-x) = 1+x$ for $x \to 0$, Eq. (6) becomes:

$$\underline{m}_s = \frac{V_s(1+\delta v_{dc}/v_{dc})}{v_{dc}} e^{j(\omega_s t+\phi)}$$

Ideally, we want the applied output voltage, $\underline{v}_s = \underline{m}_s v_{dc}$, to be equal to the command voltage $\underline{v}_s^* = V_s e^{j(\omega_s t+\phi)}$. However, due to the dc-voltage filtering, it becomes:

$$\underline{v}_s = (V_s + m\delta v_{dc})e^{j(\omega_s t+\phi)} \tag{7}$$

where $m = V_s/v_{dc}$ is the modulation index. Note that Eq. (7) is equivalent to Eq. (5), if:

$$\delta V_s = m\delta v_{dc} \quad ; \quad \delta\omega = 0 \quad ; \quad \delta\phi = 0$$

Therefore, filtering the dc-voltage used in normalization is equivalent to adding a component to the output voltage amplitude that is proportional to both δv_{dc} and m. This explains why this is an effective stabilization method, but it also shows the rigidity of its tuning, as it depends on the operating point (m).

Simulation Results

To illustrate this analysis, simulations were performed in the Matlab/Simulink environment on a VSD model with a dc-link resonance at 1.2kHz ($C_{dc} = 12.5\mu F,\ L_{dc} = 1.4mH$). In a slim-capacitance VSD supplied with a 50Hz grid, the 1.2kHz harmonic is naturally present in the dc-voltage due to the three-phase rectification process. Hence, the resonance is continuously excited. Moreover, as a worst case scenario, the damping is neglected ($R_{dc} = 0$) in the simulation, which makes the resonance even more visible.

The following use case is considered: the VSD is driving a 4kW/50Hz induction motor, using Indirect Field-Oriented Control (FOC) with 50Hz bandwidth. A speed ramp is applied up to 150% rated speed, at 80% of rated torque. Fig. 1 shows the dc-link voltage behavior when no stabilization action is applied.

Fig. 2 shows the results of dc-link stabilization when using a first-order low pass filter (LPF) on the dc-link voltage signal at 600Hz. The resonance is effectively suppressed, however the damping cannot

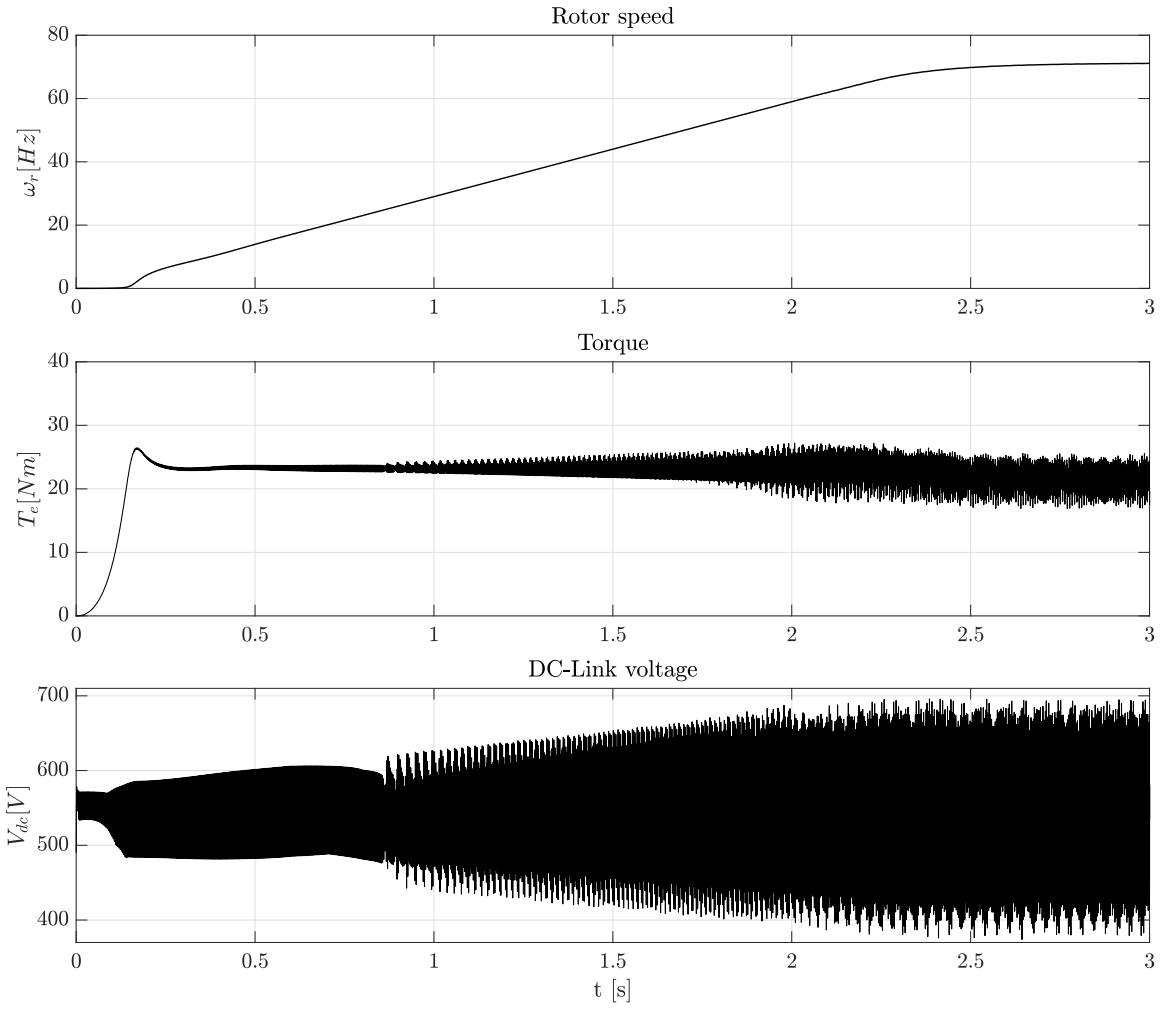

Fig. 1: DC-link resonance during acceleration

be precisely controlled at a specific operating point. The attenuation gain changes with the modulation index, which is clearly visible on the torque waveform, where the ripple amplitude increases with speed. It is possible however to roughly tune the performance by changing the filtering frequency. Choosing a higher filtering frequency, closer to the resonance, means that the naturally present harmonics in the system are not compensated in the modulation process. The consequence is lower torque ripple but higher dc-voltage ripple in all operating points.

3 Output Voltage-based Stabilization

As discussed in Section 1, direct compensation can be performed by adding the dc-link voltage ripple to the amplitude, the frequency, or the phase of the output voltage. Fig. 3 shows the implementation block diagram of the method within a VSD.

If we neglect the inverter losses, the load power can be expressed as:

$$P = \underline{i}_s^T \underline{v}_s = \frac{3}{2} V_s I_s \cos\varphi \tag{8}$$

where V_s is the peak phase voltage, I_s is the peak phase current, and $\cos(\varphi) = \cos(\phi_v - \phi_i)$ is the motor power factor. The current is the response to the voltage through the motor impedance. Therefore, when a δv_{dc} component is added to the voltage in small-signal, the current response is neglected (the higher the frequency, the higher the motor impedance). Note that if we seek a compensation mechanism that gives

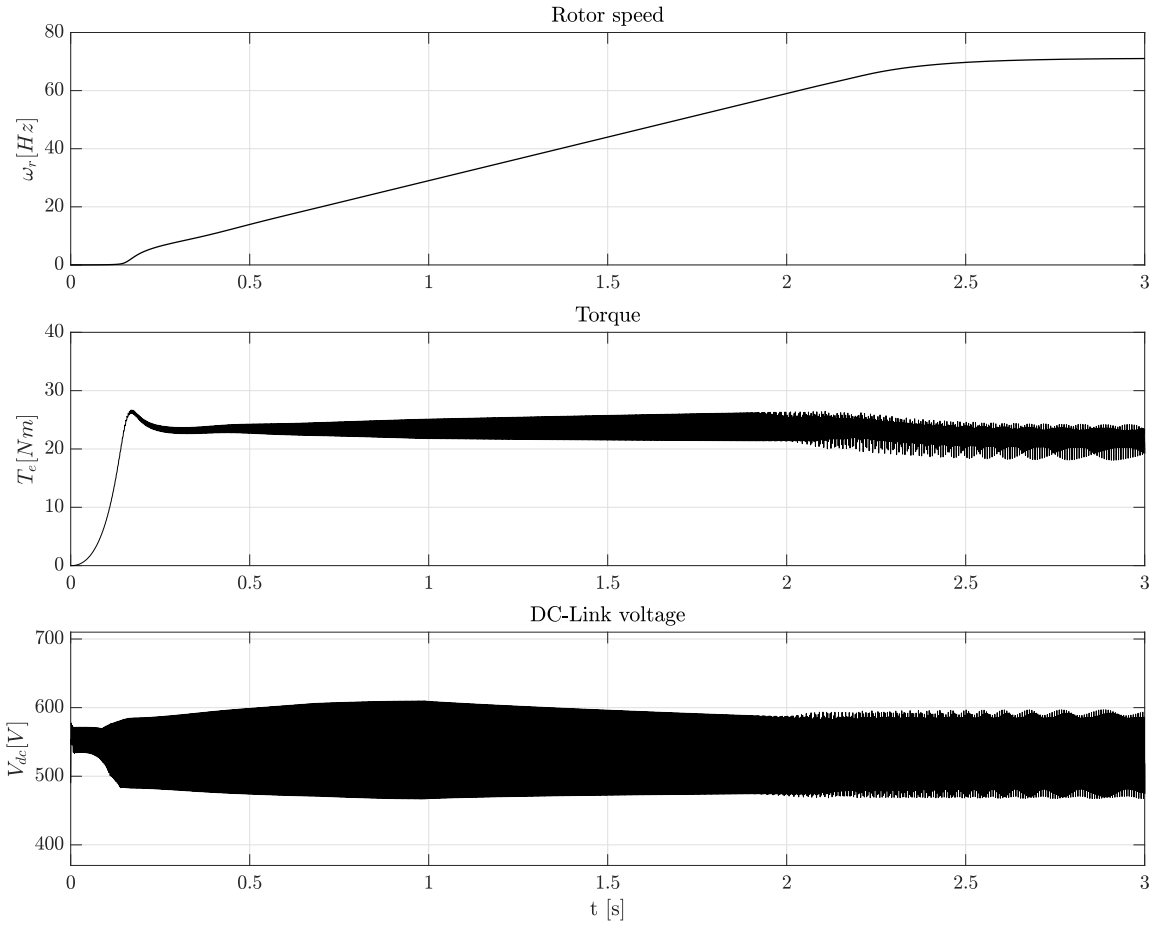

Fig. 2: DC-link stabilization by dc-link voltage filtering at 600Hz

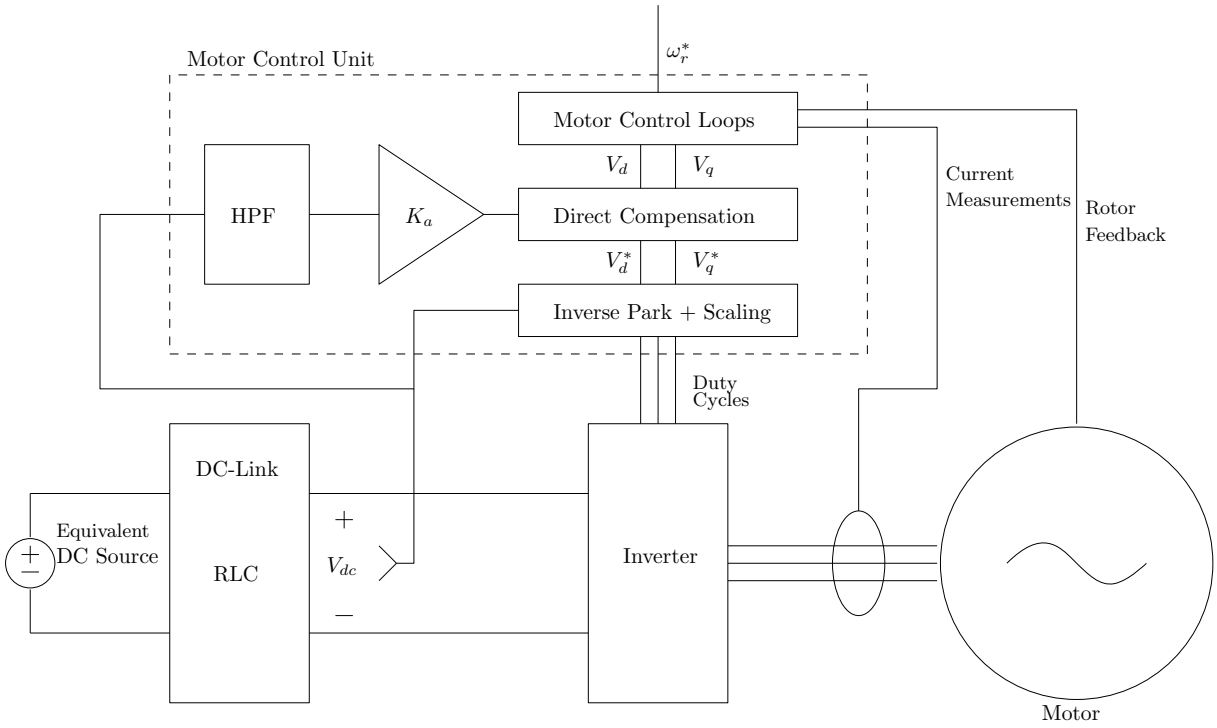

Fig. 3: Output Voltage Based Stabilization block diagram

$P = P_0 + K_a \delta v_{dc}$, only the voltage amplitude V_s and phase angle ϕ_v allow for it. Therefore, they will be thoroughly studied in the sequel. The frequency-based compensation is not in the scope of this study.

Amplitude-based Stabilization (ABS)

Using Eq. (5), amplitude-based stabilization means:

$$\delta V_s = K_v \delta v_{dc} \;\; ; \;\; \delta\omega_s = 0 \;\; ; \;\; \delta\phi_v = 0 \quad \Rightarrow \quad \underline{v_s} = (V_s + K_v \delta v_{dc})\, e^{j(\omega_s t + \phi_v)}$$

K_v is the compensation gain applied to the voltage amplitude, which is different from K_a, the resulting compensation gain on the power. This method can be implemented in the synchronous reference frame by modifying v_d and v_q in a way that changes the voltage amplitude only. This can be done as follows:

$$v_d^* = v_d + K_v \delta v_{dc} \frac{v_d}{\sqrt{v_d^2 + v_q^2}} = v_d \left(1 + \frac{K_v \delta v_{dc}}{\sqrt{v_d^2 + v_q^2}} \right) \tag{9}$$

$$v_q^* = v_q + K_v \delta v_{dc} \frac{v_q}{\sqrt{v_d^2 + v_q^2}} = v_q \left(1 + \frac{K_v \delta v_{dc}}{\sqrt{v_d^2 + v_q^2}} \right) \tag{10}$$

The verification of the above calculation can be done by evaluating:

$$V_s = \sqrt{v_d^{*2} + v_q^{*2}} \;\text{ and }\; \phi_v = \arctan\left(v_q^* / v_d^*\right)$$

Gain Tuning

The goal is to tune K_v to the value that results in the desired virtual capacitance in $K_a = C_v v_{dc0}$. From Eq. (8), the small-signal equation of the motor power can be derived as:

$$\delta P = \frac{3}{2}\left(V_{s0}\cos(\varphi_0)\delta v_s + V_{s0}\cos(\varphi_0)\delta i_s - V_{s0} I_{s0}\sin(\varphi_0)\delta\phi_v\right) \approx \frac{3}{2} I_{s0}\cos(\varphi_0)\delta v_s \tag{11}$$

With $\varphi_0 = \phi_{v0} - \phi_{i0}$. δi_s and $\delta\phi_i$ are neglected and $\delta\phi_v = 0$ by design, as only the amplitude is changed. To get $\delta P = K_a \delta v_{dc}$, with $K_a = C_v v_{dc0}$, and $\delta v_s = K_v \delta v_{dc}$, we can equate:

$$K_a \delta v_{dc} = \frac{3}{2} I_{s0}\cos(\varphi_0)\delta v_s \;\; \Leftrightarrow \;\; C_v v_{dc0}\delta v_{dc} \approx \frac{3}{2} I_{s0}\cos(\varphi_0) K_v \delta v_{dc} \;\; \Leftrightarrow \;\; K_v = \frac{2}{3}\frac{v_{dc0} C_v}{I_{s0}\cos(\varphi_0)}$$

Using this equation, and assuming $\cos\varphi_0 \approx 1$, the compensation gain tuning can be simplified:

$$K_v = \frac{2}{3}\frac{V_n C_v}{I_n} \tag{12}$$

where V_n, and I_n are respectively the rated phase voltage and the rated phase current. The gain can be easily changed by tuning the virtual capacitor's value.

Simulation results

Fig. 4 shows the ABS performance in simulation on the same setup as described in the previous section, using a 25µF virtual capacitance ($2 \times C_{dc}$), up to 150% of rated speed. The algorithm was implemented using equations (9) and (10) and a 600Hz HPF to approximate δv_{dc}. One can see that the ABS scheme has consistent performance over the whole speed range up to the voltage limitation. The damping can easily be changed by tuning K_v.

Fig. 5 shows the ABS performances with a varying gain $K_v = m$. As expected from theoretical results from section 2, this result is exactly similar to the one shown in Fig. 2.

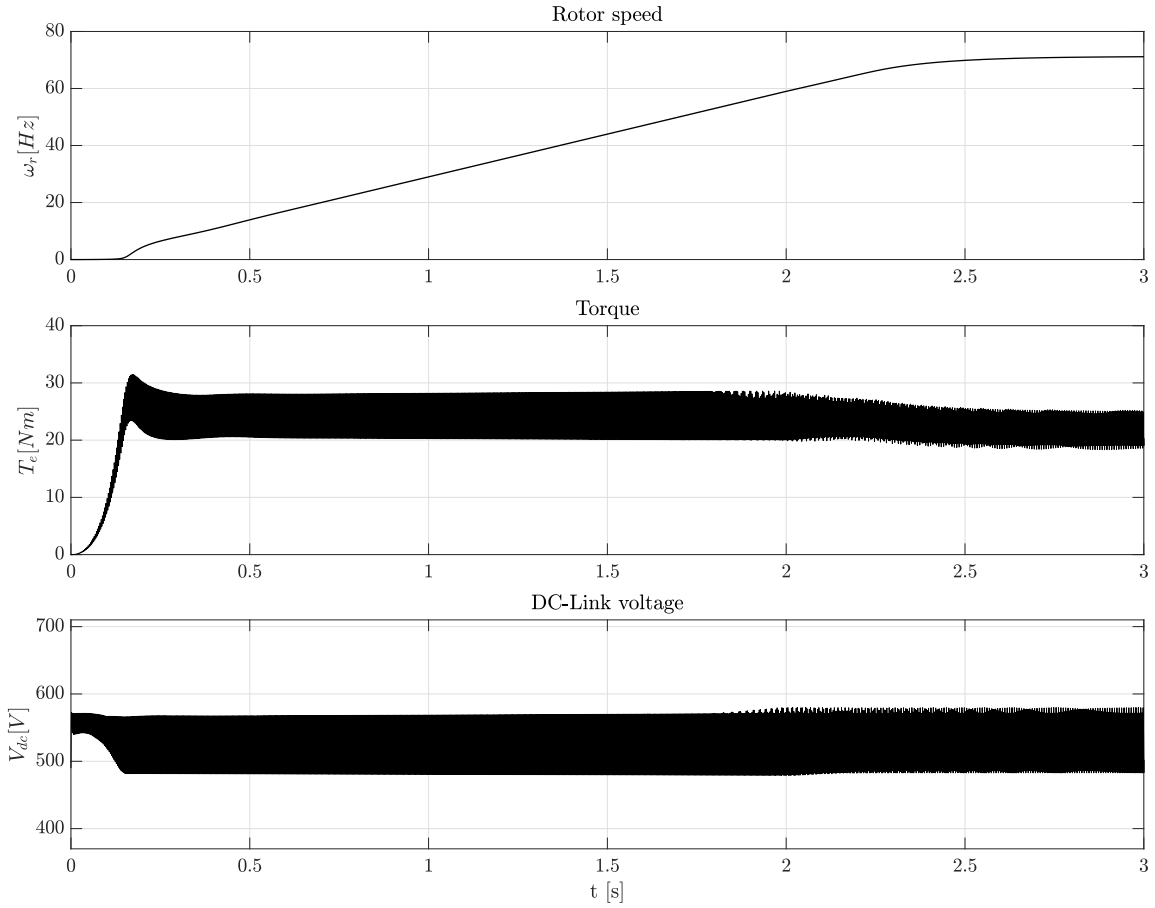

Fig. 4: ABS method performances, with $C_v = 25\mu F$ and 600Hz HPF

Phase-based Stabilization (PBS)

The ABS scheme can only be used outside of the voltage limitation region. Otherwise, the amplitude cannot be increased and the stabilization signal is not applied correctly. Nevertheless, it is possible to shape δP by acting on the voltage phase, by taking Eq. (5) and considering:

$$\delta V_s = 0 \;\; ; \;\; \delta\omega_s = 0 \;\; ; \;\; \delta\phi_v = K_\phi \delta v_{dc} \quad \Rightarrow \quad \underline{v_s} = V_s e^{j\left(\omega_s t + \phi_v + K_\phi \delta v_{dc}\right)}$$

This phase-based stabilization (PBS) method can also be implemented in the synchronous reference frame and expressed using the complex-vector notation, as follows:

$$\underline{v_s^*} = v_d^* + j v_q^* = \underline{v_s} e^{j\delta\phi} = \underline{v_s} e^{jK_\phi \delta v_{dc}} \tag{13}$$

In scalar form:

$$v_d^* = v_d \cos(K_\phi \delta v_{dc}) - v_q \sin(K_\phi \delta v_{dc}) \tag{14}$$
$$v_q^* = v_q \cos(K_\phi \delta v_{dc}) + v_d \sin(K_\phi \delta v_{dc}) \tag{15}$$

To simplify the implementation, the first order Taylor's approximation can be applied, as the angle oscil-

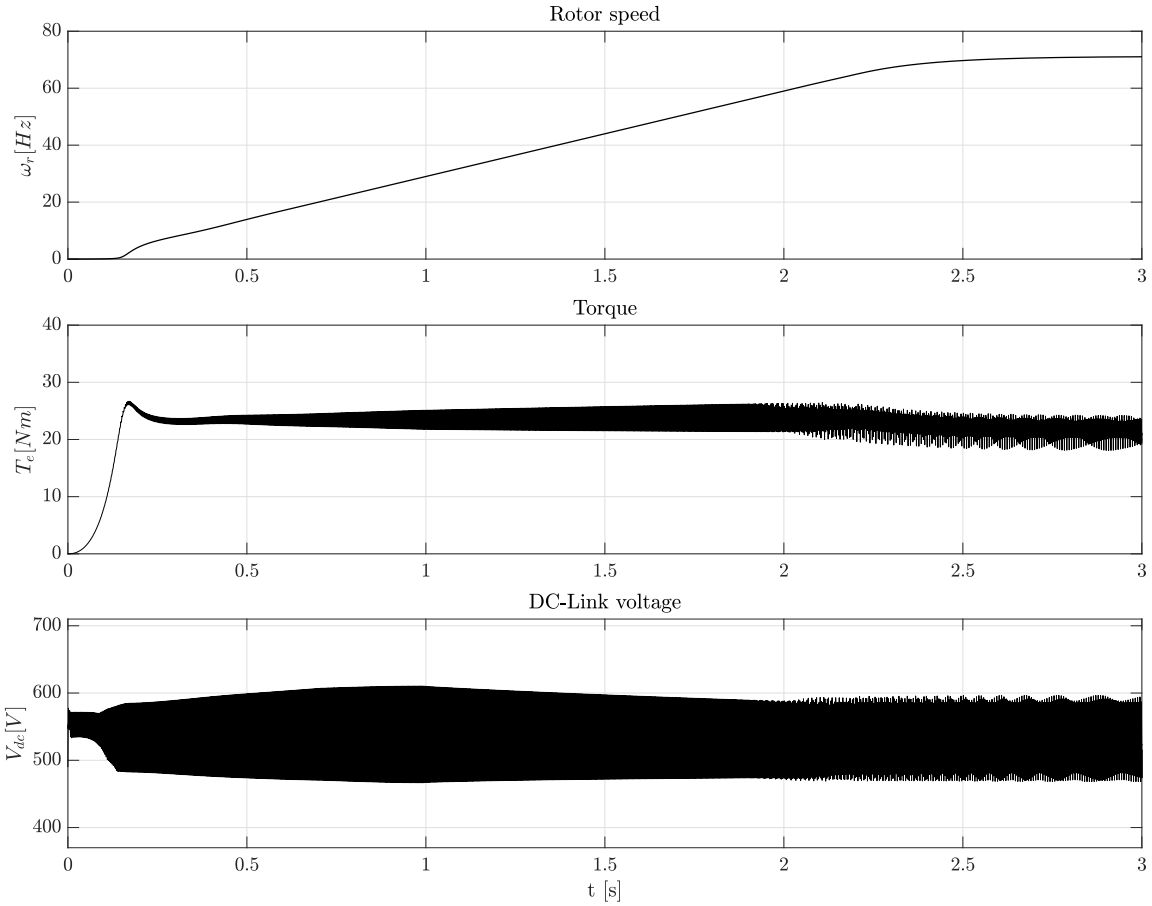

Fig. 5: ABS with $K_v = m$ and 600Hz HPF

lation should be small, $e^{jK_\phi \delta v_{dc}} \approx (1 + jK_\phi \delta v_{dc})$. This gives:

$$v_d^* = v_d - v_q K_\phi \delta v_{dc} \tag{16}$$

$$v_q^* = v_q + v_d K_\phi \delta v_{dc} \tag{17}$$

It is not advised to use the above approximation outside of the voltage limitation region. The voltage circle is smaller for lower voltage amplitudes, and the first order approximation loses precision. Performances with this method will be highest when the applied voltage is at its maximum value.

Gain Tuning

The gain K_ϕ links δP to $\delta\phi$. It can be calculated using the same approach of K_v and the virtual capacitance concept:

$$\delta P = \frac{3}{2}(V_{s0}\cos\varphi_0 \delta v_s + V_{s0}\cos\varphi_0 \delta i_s - V_{s0} I_{s0}\sin\varphi_0 \delta\phi_v) \approx -\frac{3}{2} V_{s0} I_{s0}\sin\varphi_0(\delta\phi_v) \tag{18}$$

with $\delta v_s = 0$ by design and δi_s neglected, which gives:

$$K_\phi = -\frac{2}{3}\frac{C_v v_{dc0}}{V_{s0} I_{s0}\sin(\varphi_0)} \approx -\frac{2}{\sqrt{3}}\frac{C_v}{I_n \varphi_0} \tag{19}$$

Note that K_ϕ is negative because of the inverse influence of the voltage phase on the electrical power in small-signal.

Full-range stabilization

Both amplitude-based stabilization (ABS) and phase-based stabilization (PBS) are combined to provide satisfactory performance over the complete operation range. To avoid a discontinuity when switching between methods, a progressive smooth transition has been implemented:

$$\underline{v_s} = (V_s + (1-\alpha)K_v\delta v_{dc})e^{j\left(\omega_s t + (\phi_v + \alpha K_\phi \delta v_{dc})\right)} \tag{20}$$

Where $\alpha \in [0,1]$ is a coefficient that is calculated based on the instantaneous value of V_s:

$$\begin{cases} \alpha = 0\ , & V_s < V_1 \\ \alpha = \dfrac{V_s - V_1}{V_2 - V_1}\ , & V_1 < V_s < V_2 \\ \alpha = 1\ , & V_s > V_2 \end{cases} \tag{21}$$

In a conventional VSD (with smooth dc-voltage), the voltage limitation region is reached close to the rated voltage, so V_1 could be set at 90% and V_2 at 95% for example. In slim-capacitor VSDs, the voltage oscillates continuously between 86% and 100% of the grid line-line voltage. In this case, V_1 is set to 80% and V_2 to 85% of the rated motor voltage.

Fig.6 shows the performances of the combined ABS-PBS method, up to 150% of rated speed. Results show that, compared to the ABS alone (see Fig.4), the combined method has superior performances in the voltage limitation region. The DC-link voltage resonance is suppressed and torque ripples are largely dampened in the field-weakening region.

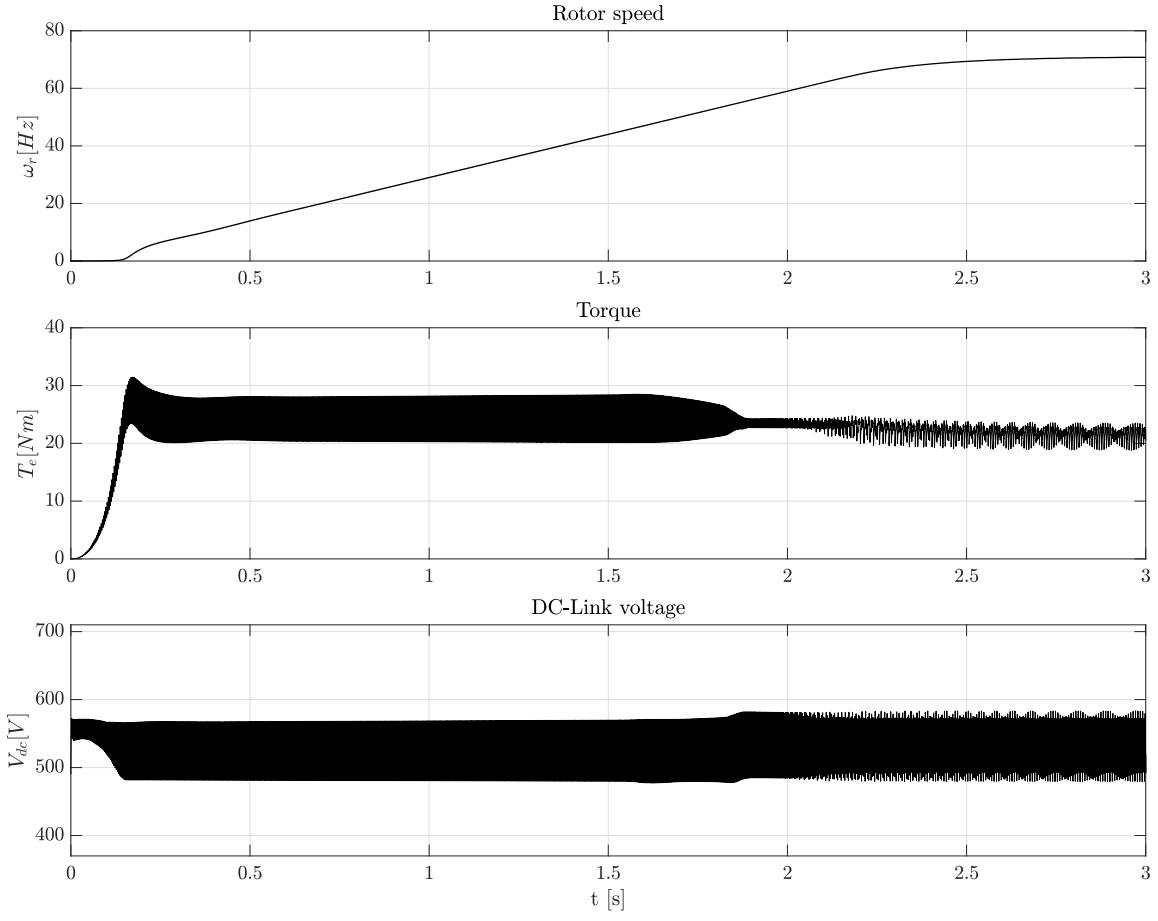

Fig. 6: Combined ABS-PBS method, with $C_v = 25\mu F$ and 600Hz HPF

4 Conclusion

In this paper, direct active stabilization of the dc-link oscillation has been studied. First, the dc-voltage filtering-based method was analyzed. It was shown that its small-signal behavior is equivalent to compensating the output voltage amplitude proportionally to the modulation index. This effective yet rigid method can be outperformed by the combination of two new direct methods: voltage amplitude-based stabilization and voltage phase-based stabilization. These methods are easy to implement in the synchronous reference frame, they require slightly more calculations than the voltage filtering method which is the cost of improved performance and superior tuning capability. This being said, the calculation burden of the proposed method remains low compared to other state-of-the-art methods.

The virtual capacitor concept is very useful to tune the stabilization gain. These methods were tested and compared in simulation. The frequency-based stabilization method was not analyzed in this paper, which can be the topic of future work.

References

[1] S. D. Sudhoff, K. A. Corzine, S. F. Glover, H. J. Hegner and H. N. Robey, "DC link stabilized field oriented control of electric propulsion systems," in IEEE Transactions on Energy Conversion, vol. 13, no. 1, pp. 27-33, March 1998

[2] M. Koteich, "Stability Analysis of a DC-link with Nonlinear Load – An Overview," 2021 23rd European Conference on Power Electronics and Applications (EPE'21 ECCE Europe), 2021, pp. P.1-P.11.

[3] D. Marx, P. Magne, B. Nahid-Mobarakeh, S. Pierfederici and B. Davat, "Large Signal Stability Analysis Tools in DC Power Systems With Constant Power Loads and Variable Power Loads—A Review," in IEEE Transactions on Power Electronics, vol. 27, no. 4, pp. 1773-1787, April 2012

[4] W. Lee and S. Sul, "DC-Link Voltage Stabilization for Reduced DC-Link Capacitor Inverter," in IEEE Transactions on Industry Applications, vol. 50, no. 1, pp. 404-414, Jan.-Feb. 2014

[5] K. Pietilainen, L. Harnefors, A. Petersson and H. -. Nee, "DC-Link Stabilization and Voltage Sag Ride-Through of Inverter Drives," in IEEE Transactions on Industrial Electronics, vol. 53, no. 4, pp. 1261-1268, June 2006

[6] O. Wallmark, S. Lundberg and M. Bongiorno, "Input Admittance Expressions for Field-Oriented Controlled Salient PMSM Drives," in IEEE Transactions on Power Electronics, vol. 27, no. 3, pp. 1514-1520, March 2012

[7] J. Koppinen and M. Hinkkanen, "Impact of the switching frequency on the DC-side admittance in three-phase converter systems," 2014 16th European Conference on Power Electronics and Applications, 2014, pp. 1-10

[8] H. Mosskull, "Stabilization of an induction motor drive with resonant input filter," 2005 European Conference on Power Electronics and Applications, 2005, pp. 10 pp.-P.10

[9] Y. A. I. Mohamed, A. A. A. Radwan and T. K. Lee, "Decoupled Reference-Voltage-Based Active DC-Link Stabilization for PMSM Drives With Tight-Speed Regulation," in IEEE Transactions on Industrial Electronics, vol. 59, no. 12, pp. 4523-4536, Dec. 2012

[10] T. Devos and P. Martin, "Avoiding DC link oscillations in drives," IECON 2020 The 46th Annual Conference of the IEEE Industrial Electronics Society, 2020, pp. 876-882

[11] M. Hinkkanen and J. Luomi, "Induction Motor Drives Equipped With Diode Rectifier and Small DC-Link Capacitance," in IEEE Transactions on Industrial Electronics, vol. 55, no. 1, pp. 312-320, Jan. 2008, doi: 10.1109/TIE.2007.903959.